5.2 INVESTIGATING POSSIBLE CAUSATIVE MECHANISMS BEHIND THE HOUSTON CLOUD-TO-GROUND LIGHTNING ANOMALY

Michael L. Gauthier* and Walter A. Petersen
The University of Alabama in Huntsville, Huntsville, Alabama

1. INTRODUCTION

Anthropogenic influences such as the Urban Heat Island (UHI) and increased aerosol concentrations have been postulated for many years to have an effect on lower tropospheric chemistry, convection, lightning and rainfall (e.g., Huff and Changnon 1973; Westcott 1995, Jauregui and Romales 1996; Rosenfeld and Lensky 1998; Bornstein and Lin 2000; Shepherd et al. 2002; Rosenfeld and Woodley 2003). Moreover, these influences have been invoked as possible explanations for the cloud-to-ground (CG) lightning anomalies observed over the Houston metropolitan area. In particular, Orville et al. (2001) and Steiger et al. (2002) reported a 45% increase in annual CG lightning flash densities over and downwind of the Houston urban corridor relative to rural surroundings citing anthropogenic influences as possible causative mechanisms. Extending these findings, Gauthier et al. (2005) demonstrated that in a regional context the Houston CG lightning anomaly is a non-unique feature, embedded within the larger-scale enhancement of CG lightning along the Texas and Louisiana Gulf Coast (see Figure 1). Despite the fact that the Houston area is located at the western edge of this coastal enhancement, Gauthier et al. found this anomaly to be a persistent summer-season feature (even when large lightning events were excluded from the analysis) with flash densities over and downwind of the Houston metropolitan area on the order of 1.5-2 times that of it's immediate surroundings.

Interestingly, these particular types of urban signals in CG lightning activity have also been noted downwind of other cities in the U.S. and abroad (e.g. Westcott, 1995; Soriano and Pablo, 2002; Naccarato et al. 2003). Although neither new, nor individually unique to the Houston area, the primary hypotheses offered to explain the localized enhancement in summer-season CG lightning revolve around "urban" effects. Broadly stated, the hypotheses can be summarized as follows: 1) ***UHI thermodynamics*** provide a more favorable environment for convective initiation and thunderstorm intensification over and downwind of the Houston urban area resulting in more lightning activity and heavier precipitation (Huff and Changnon 1973); 2) UHI-forced convergence and associated ***mesoscale enhancements in sea breeze convergence***, simply cause more frequent convection, and associated precipitation and lightning activity over the city (Braham et al. 1981; Hjelmfelt 1982); and 3) ***urban aerosol loading***, particularly enhanced cloud condensation nuclei (CCN) concentrations in polluted air masses may contribute to the suppression of the mean droplet size, delaying the onset of the collision-coalescence process thereby making more cloud water available to colder cloud regions where it would be operative in the charge generation process resulting in enhancements in CG lightning (Rosenfeld and Lensky 1998; Rosenfeld 1999, 2000; Rosenfeld and Woodley 2000 and Williams et al. 2002).

The intent of this paper is to isolate and address the feasibility of each of the above hypotheses (also referred to as climatologically "forcing-functions") in explaining the ***climatological*** summer-season lightning anomaly over the Houston area by examining how flash density characteristics change through the selective exclusion of relevant subsets of the data (i.e. days in which a strong UHI is observed, high pollutant days, etc.) from subsequent calculations.

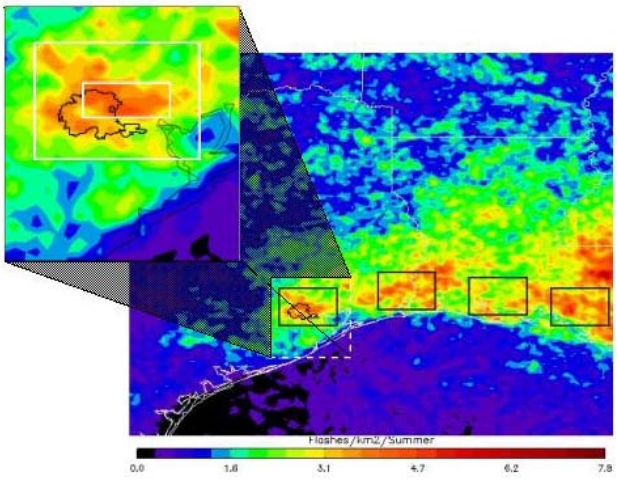

Figure 1. Spatial variations of the 8-year mean summer season (JJA, 1996-2003; valid 0900-1859 CST) ground flash density, with the Houston metropolitan area outlined in black. Black boxes in the larger image denote areas used in the determination of statistically "large" lightning days (described in the Appendix) while the dashed white box over the Houston area corresponds to the zoomed portion of the image, depicting the CAMS domain discussed in section 2.2; inner white box within the CAMS domain represents the Houston "Anomaly" box, while outer white box depicts the Houston "area", both referenced in the text.

*Corresponding author address: Major Michael L. Gauthier, Dept. of Atmospheric Science, Univ. of Alabama in Huntsville, Huntsville, AL 35899, e-mail: Michael.Gauthier@msfc.nasa.gov. *The views expressed in this paper are those of the author and do not reflect the official policy or position of the U.S. Air Force, Dept. of Defense or the U.S. Govt.*

2. DATA AND METHOD

To investigate the feasibility of each of the outlined hypotheses, this study utilized data from three separate archived datasets spanning the summer months (June, July and August; JJA) of 1996 - 2003: (1) CG lightning data from the National Lightning Detection Network (NLDN), (2) surface wind and temperature data and (3) sulfur-dioxide (SO_2) measurements, a proxy for CCN concentrations.

Each dataset was used to establish the long-term spatial and temporal variations for each of the respective observables (i.e. climatologies). Further, the individual datasets were quantitatively filtered and merged into a single composite in which four specific classifiers could be associated with each resident day. Specifically, of the 736 summer days, there were 527 days in which each of the following could be established / calculated:

(1) Hourly and daily flash counts over the Houston area
(2) Sea-breeze classification (active 'SB' or not 'noSB')
(3) Intensity of urban heat island (UHI – urban heat island index)
(4) Intensity of pollutant concentration (AI – aerosol index)

Following daily classifications, we examined how flash density characteristics over the Houston area changed through the selective exclusion of relevant subsets of the data (i.e. "Large" UHI days, "Large" AI days, etc) from subsequent flash density calculations.

2.1 Cloud-to-Ground Lightning Dataset

As the premise for this study is the existence of a persistent summer-season (JJA) anomaly in ground flash densities over the Houston metropolitan area, we will use NLDN CG lightning data (Cummins et al., 1998) as our primary dataset. Through a process of selective exclusion (outlined above) we will ascertain, and control for, the relative contributions of each of the proposed hypotheses on the flash density characteristics over and around the Houston area using changes in the mean flash densities over: (1) the Houston urban area, and (2) the Houston "anomaly" box as our metrics (zoomed portion of Figure 1, large white box and inner white box, respectively).

To that end, a series of regional total ground flash density climatologies, each valid 0900-1859 CST (horizontal resolution of 0.05^o latitude x longitude) were generated with periods of record (PORs) ranging from 736 days (8 summer-seasons x 92 days/summer) to a final baseline of 336, non-contiguous, days in which synoptic conditions were quantitatively determined to be favorable for the formation of a sea-breeze circulation (described in the Appendix). In constructing these climatologies we have chosen to focus our attention on ground flashes occurring during daylight hours as it is during this time in which each of the hypothesized forcing mechanisms are expected to have their greatest impacts, further it is during this time of the day that greater than 70% of the CG lightning occurs over the Houston area. Further, we have disregarded flashes with positive peak currents less than 10 kA following the recommendations of Cummins et al. (1998) and Wacker and Orville (1999a,b).

2.2 Meteorological and Pollutant Datasets

As detailed in the Appendix, each of the days in our final overlapping dataset were quantitatively classified as either a "Sea Breeze" (SB) or "Non-Sea Breeze" (noSB) day, each of these days were also assigned urban heat island and aerosol indices (UHI and AI, respectively). Hourly surface measurements of temperature, winds (speed and direction), and pollutant concentrations (i.e. Sulfur-dioxide (SO_2), explained later) for these quantitative classifications came primarily from a network of Continuous Ambient Monitoring Stations (CAMS) operated by the Texas Commission on Environmental Quality (TCEQ), with supplementary upper air information extracted from NCEP/NCAR Reanalysis data. Figure 2a depicts the locations of the 35 CAMS meteorological monitoring sites (11 of which also provide mean hourly measurements of SO_2; blue numbers in Figure 2) used in this study.

2.2.1 Meteorological Analysis

In constructing our spatial climatologies for each of the meteorological variables, mean hourly climatologies were first generated for each individual site. Once site-specific hourly climatologies were generated, the analysis area (depicted in Figure 2) was divided into a 29 x 36 Cartesian grid with horizontal resolution of 0.041^o (latitude x longitude), with the mean hourly data interpolated onto the grid using a Cressman-Barnes objective analysis method (Barnes 1964). The result of this analysis is a series of hourly maps depicting the spatial variations of mean temperatures and wind vectors; for further comparison, mean hourly divergence fields were calculated from the gridded velocity vectors.

2.2.2 Pollutant Analysis

Past studies attempting to correlate enhancements in CG lighting activity to anthropogenic effects have used measurements of different aerosol tracers as gross indicators of pollutant levels and CCN concentrations. Most notably, researchers have attempted to use measurements of annual means of PM_{10} (particulate matter with aerodynamic diameters smaller than 10 microns) and Sulfur-dioxide (SO_2) as the tracers of choice in their analyses (i.e. Westcott, 1995, Steiger et al., 2002, Soriano and Pablo, 2002 and Naccarato et al., 2003).

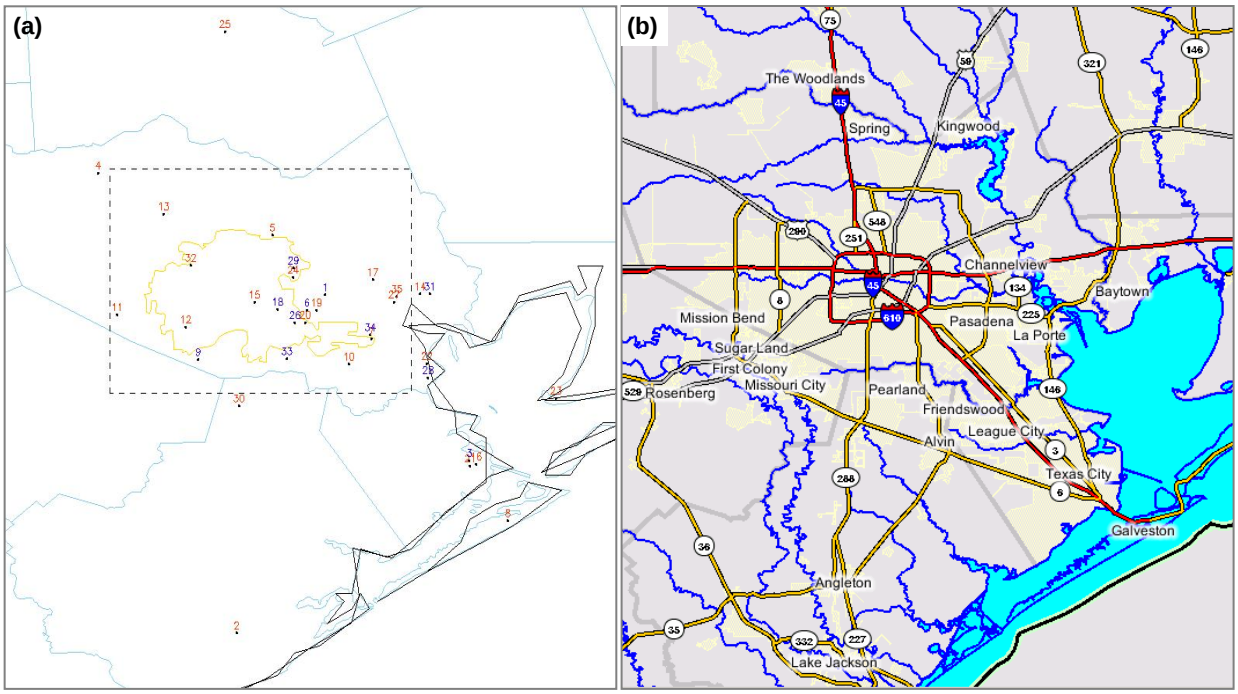

Figure 2. (a) Location of 35 Continuous Ambient Monitoring Stations (CAMS) operated by the Texas Commission on Environmental Quality (TCEQ) providing mean hourly surface measurements of temperature and winds (speed and direction); sites number in blue also provide mean hourly measurements of SO_2 concentrations. (b) Detailed map of the CAMS analysis area depicting the location of major roadways as well as prominent water features throughout the area.

Although archived data is available from the Environmental Protection Agency (EPA) for PM_{10} and SO_2, temporal resolutions are insufficient for use in this study (only daily means available, every eighth day for PM measurements), therefore we have chosen to use available mean hourly measurements gathered by CAMS sites to form our complementary pollutant analysis. Specifically, we use SO_2 (vice $PM_{2.5}$, particulate matter with aerodynamic diameters smaller than 2.5 microns) as our tracer of choice as hourly SO_2 measurements are available throughout the entire POR ($PM_{2.5}$ data is only available from 2001-2003). As further justification for this choice, we note a positive correlation between the time-averaged mean $PM_{2.5}$ and SO_2 observations at a common site with a correlation coefficient (r) of 0.70, indicating that approximately 50% of the variance in mean $PM_{2.5}$ measurements can be explained by the variance in mean SO_2 measurements.

The methodology applied to the gridding of the temperature and wind fields described in section 2.2.1 was also applied to our pollutant analysis, resulting in hourly maps depicting the spatial distribution of SO_2 concentrations.

2.3 Data Filtration – the use of Selective Exclusion (SE) Filters

To explore the aforementioned hypotheses the merged dataset was filtered so as to isolate each of the three forcing-functions (sea breeze, enhanced UHI, and enhanced AI) from the other two, thereby allowing a direct assessment of the contribution of each variable to the long-term CG lightning climatology. Specifically, using the statistical distributions of each variable within the merged dataset, the following quantitative filters were developed (see Appendix for complete descriptions):

SE1 - large lightning event day filter
SE2 - sea breeze day filter (includes 6 sub-filters)
SE3 - “large” UHI day filter
SE4 - “large” AI day filter

The application of SE1 and the first half of SE2 (i.e. filters 1-3) further reduced the 527 day dataset to 336 distinct days, conditioned on the absence of statistically large lightning event days (i.e. the extreme/outlier events), each with similar background synoptic conditions favorable for the formation of a thermally driven sea breeze circulation. That is to say our 336 day dataset is one that reproduces the general features of the long-term mean CG lightning climatology (compare zoomed portion of Figure 1 with Figure 3, note difference in contour intervals), while allowing for the potential development of a sea breeze circulation; it is the application of the remainder of SE2 (i.e. filters 4-6) that will ultimately determine the sea breeze classification for each day.

Subsequent to the application of the four SE filters, the final dataset is composed of the following isolated days (i.e. only one of the hypothesized enhancements are present a given day): 62 sea breeze days, 57

"large" or enhanced UHI days, 48 enhanced AI days and 116 non-enhanced days (i.e. none of the hypotheses could be tested, as defined). These 116 non-enhanced days comprise the "background" to which each of the enhancements are be added to reconstruct the final climatology.

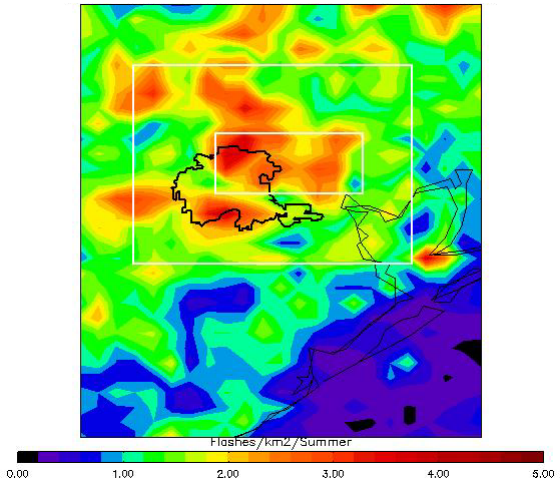

Figure 3. Spatial variations of mean flash density (valid 0900-1859 CST) for 336 non-contiguous days resulting from the application of SE1 and the first half of SE2. Domain and spatial references correspond to zoomed portion of Figure 1.

3. RESULTS AND DISCUSSION

As previously outlined, this study has two primary components, (1) establishment of component climatologies and (2) filtering of the conditioned dataset through a process of selective exclusion, the results of both will be discussed herein.

3.1 *Component Climatologies*

Overlaying the various climatologies upon one another provides a useful tool for the identification of potential "forcing-response" relationships that may exist within the long-term mean (i.e. enhanced UHI forcing resulting in the atmospheric response of enhanced CG lightning activity). The results of this effort are presented in a series of spatial composites (Figures 4a-e), as well as in the form of a composite time series of mean values observed over the Houston urban area (Figure 5). For clarity, in Figure 4 we have contoured total hourly flash densities using a grayscale, and have chosen a color scale to represent areas of convergent flow only (i.e. divergence is not presented). Additionally, only wind vectors in excess of 2.5 m/s have been overlaid, with thermal anomalies (defined here as the mean hourly pixel temperature reduced by the mean hourly temperature of the entire domain) contoured in red every 0.5^{o}F beginning at 2.5^{o}F.

Throughout the predawn hours, warmer surface temperatures reside over the water with predominantly southerly flow and stronger surface winds located at coastal locations. Additionally, various areas of enhanced convergence, particularly one over north-central Houston are also present, with nominal enhancements in mean SO_2 concentrations near the mouth of Galveston Bay. As would be expected, climatological lightning activity appears insignificant over land, with only minimal enhancements located near the mouth of Galveston Bay. By 0600L (Figure 4a) surface winds have bottomed out throughout the domain, with only a minimal onshore component. At this point, warmer temperatures continue to exist over the water, with no apparent sign of organized lightning activity as of yet. Initial enhancement in pollutant concentrations also becomes apparent over the central portions of the city, likely associated with the onset of commuter activity coupled with industrial emissions occurring during a time when the stable (shallow) nocturnal boundary layer has yet to erode. Following sunrise, the next 3 hours see an increase in surface wind speeds, becoming predominantly southerly, with the beginnings of an enhanced UHI over north-eastern Houston along with peak SO_2 concentrations located over the industrialized portions of the city (see Figure 4b; valid 0900L). By local noon (Figure 4c) we see that the UHI has expanded over the central portion of the urban domain and has intensified significantly, further enhancing the area of low-level convergence located over the north-eastern portions of the city with aerosol concentrations decreasing, likely due to dilution associated with physical mixing (encroachment of the SB) along with rainout and a deepening of the convective boundary layer. Organized lightning activity becomes apparent along the leading edge of the sea breeze front, still predominantly outside the confines of the city. Figure 4d, one hour later, illustrates the atmospheric response to the localized forcing due to the enhanced UHI over the north-central portion of the city. Here the atmosphere responds to the intense UHI with a continued intensification of surface wind convergence and more importantly, a strong response in convective activity with mean hourly flash densities nearing the maximum within the domain during this timeframe. Following this initial pulse in lightning activity at 1300L, convection appears to become more organized, propagating from the northwestern tip of Galveston Bay over the Houston area (particularly the area of the strongest UHI) where it intensifies, followed by a subsequent cessation in activity as it departs the favorable convergence zone (see Figure 4e; valid 1500L). By this time we note further decreases in aerosol concentrations over the city, with increases at coastal locations, a testament to our earlier statement where we speculated that continuous emissions throughout the day are diluted over the urban area likely due to precipitation scavenging and rainout processes coupled with a deeper CBL, compared to cooler coastal regions where we would expect a more stable, shallower boundary layer to exist. At this time, the increased surface roughness within the city, associated with the presence of buildings and other structures is

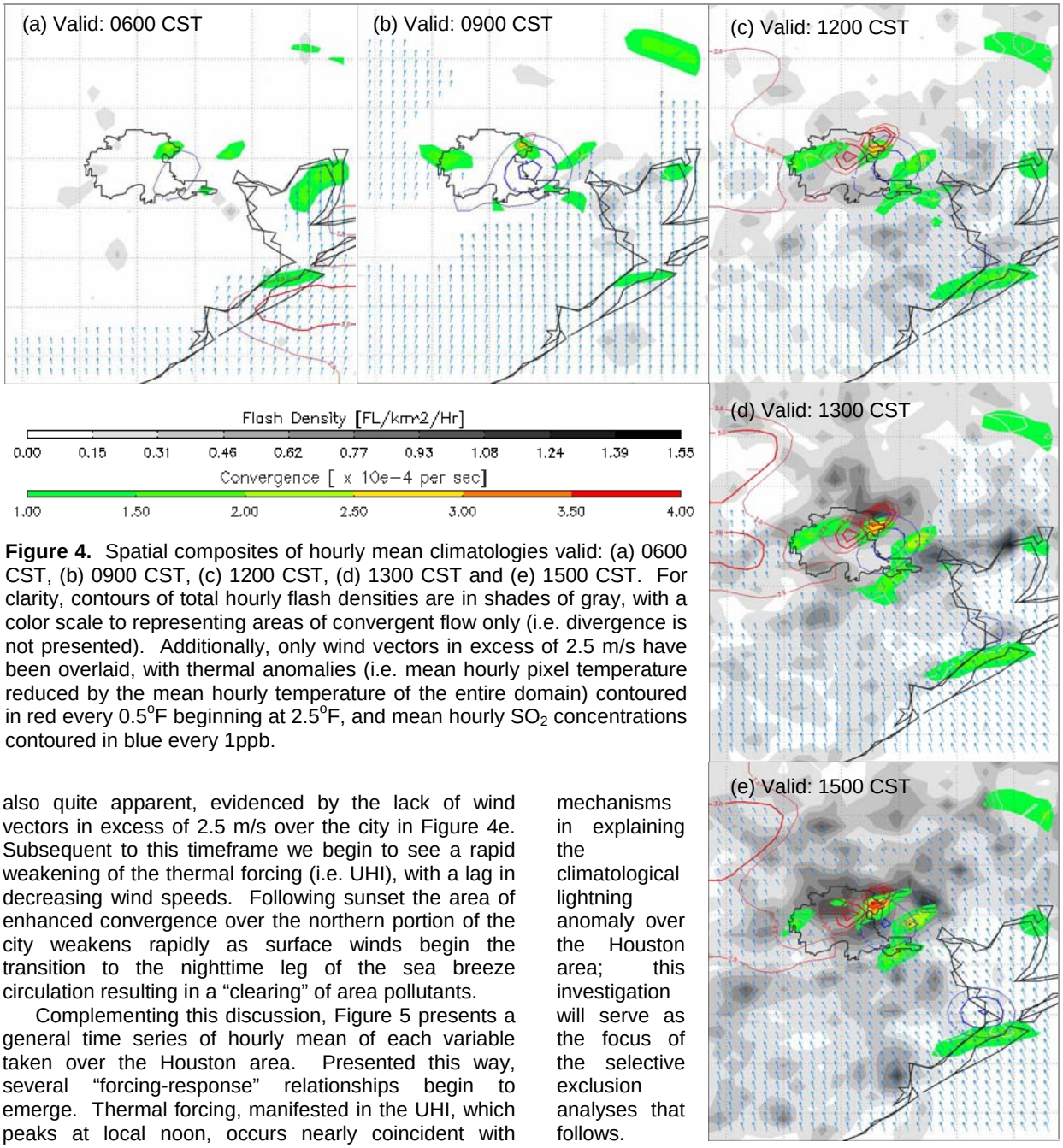

Figure 4. Spatial composites of hourly mean climatologies valid: (a) 0600 CST, (b) 0900 CST, (c) 1200 CST, (d) 1300 CST and (e) 1500 CST. For clarity, contours of total hourly flash densities are in shades of gray, with a color scale to representing areas of convergent flow only (i.e. divergence is not presented). Additionally, only wind vectors in excess of 2.5 m/s have been overlaid, with thermal anomalies (i.e. mean hourly pixel temperature reduced by the mean hourly temperature of the entire domain) contoured in red every 0.5°F beginning at 2.5°F, and mean hourly SO_2 concentrations contoured in blue every 1ppb.

also quite apparent, evidenced by the lack of wind vectors in excess of 2.5 m/s over the city in Figure 4e. Subsequent to this timeframe we begin to see a rapid weakening of the thermal forcing (i.e. UHI), with a lag in decreasing wind speeds. Following sunset the area of enhanced convergence over the northern portion of the city weakens rapidly as surface winds begin the transition to the nighttime leg of the sea breeze circulation resulting in a "clearing" of area pollutants.

Complementing this discussion, Figure 5 presents a general time series of hourly mean of each variable taken over the Houston area. Presented this way, several "forcing-response" relationships begin to emerge. Thermal forcing, manifested in the UHI, which peaks at local noon, occurs nearly coincident with increases in wind speeds, both intensity and onshore component, thereby leading to enhanced convergence over the Houston metropolitan area (1400L) followed by peak mean hourly flash densities (1500L; the ultimate atmospheric response). The time lag between peaks for each of these variables strongly indicates the presence of a physical forcing-response relationship. Another, yet to be explored, relationship may exist between mean hourly SO_2 concentrations over the city and enhanced flash densities. Here, mean hourly flash densities appear to lag peaks in mean hourly SO_2 concentrations by about 5 hours. It is important to note, however, that some, all or none of these forcing-response relationships may prove to be predominant causative mechanisms in explaining the climatological lightning anomaly over the Houston area; this investigation will serve as the focus of the selective exclusion analyses that follows.

3.2 Apportioning the Cause – Selective Exclusion Filtration

The results of the first portion of this study have firmly established the existence of possible climatological "forcing functions" that may be capable of explaining the observed climatological enhancement in CG lightning activity over the Houston area. What remains is to determine which, if any, of the proposed hypotheses can be deemed the primary causative mechanism, or more likely which, if any, can be

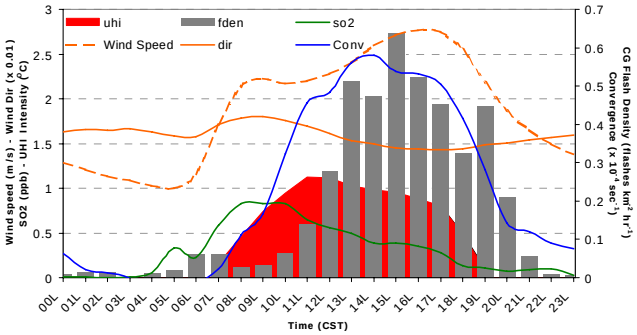

Figure 5. Diurnal time series of the spatial hourly means for the following parameters, each computed over the Houston area (i.e. outer white box in Figure 3): UHI intensity (red shading), mean wind speed and direction (orange lines), mean hourly convergence over the Houston area (blue line), mean hourly SO2 concentrations (green line) and mean hourly flash densities (gray bars).

eliminated as a predominant contributor. To that end, the second portion of this study focuses on determining the relative contributions that each of the proposed hypotheses have on the Houston CG lightning anomaly through the selective exclusion of relevant subsets of the data.

As previously discussed, SE1 and the first portion of SE2 (filters 1-3) were utilized to filter and condition the original 786 day dataset down to 336 distinct non-consecutive days for inter-comparison, each conditioned upon the existence of favorable synoptic conditions for the formation of a sea breeze circulation. From this analysis we define our baseline metrics as the mean flash densities over the Houston area (outer box in Figure 6a) as well as within the Houston "anomaly" box (inner box, same figure). Specifically, the values against which subsequent analyses will be compared are 1.88 and 2.49 ("anomaly" box) flashes km^{-2} $summer^{-1}$.

Examining the results of the application of the remainder of SE2 (identification of SB and noSB), SE3 (exclusion of "Large" UHI days) and SE4 (exclusion of "Large" AI days) to the conditioned dataset, there are a total of 169 days that were not dominantly influenced by any of the defined "forcing functions" – these days will comprise the background value, to which each of the isolated forcing functions can be added to examine how they particularly enhance the spatial flash density distributions. The dataset is comprised of the following isolated days with associated contributions to the mean flash density metrics just described (the sum of which construct the climatology presented in Figure 6a; summarized in Table 1), contributions to the "anomaly" box are presented in parentheses: 169 non-enhanced days contributing 52% of the total CG lightning over the Houston area (61% over the anomaly box), followed by 57 enhanced UHI days contributing 25% (20%) of the mean, 62 SB days contributing 18% (13%), and 48 enhanced AI day providing the remaining 6% (7%) of the mean flash densities over the Houston area.

Spatially, the 169 non-enhanced days comprising the background provide the foundation for areas of enhanced flash densities over the northern periphery of the city (on the order of 50-60% of the total mean), and a finger of enhanced flash densities extending ENE from northeastern boundaries of the urban area (60-70% of the mean) and to a lesser extent an area of activity along the central southern boundary of the city (Figure 6b). Absent the hypothesized forcing functions, we conclude the presence of these features to be associated with "typical" convective storms driven by (1) normal diurnal forcing (i.e. the presence of a typical UHI over the north central portions of the city giving rise to an area of preferred convective initiation and/or enhancement) and (2) local topography, as opposed storms occurring on days in which enhanced forcing is present. That is not to say that the intensity of these features will not be strengthened through enhanced

	Synoptically Conditioned Days (IAH Box)	Synoptically Conditioned Days ("Anomaly" Box)
Total Number of Days	***336***	***336***
Mean Flash Denisty (FDEN - all days in dataset)	1.88118	2.49478
Number of Isolated Non-enhanced Days	***169***	***169***
Mean FDEN Non-enhanced Days	0.981339	1.52188
Mean Contribtion to FDEN over IAH	52%	61%
Number of Isolated SB Days	***62***	***62***
Mean Flash Density SB Days	0.32998	0.31262
Mean Contribtion to FDEN over IAH	18%	13%
Number of Isolated Enhanced UHI Days	***57***	***57***
Mean FDEN Enhanced UHI Days	0.462372	0.487688
Mean Contribtion to FDEN over IAH	25%	20%
Number of Isolated Enhanced AI Days	***48***	***48***
Mean FDEN Enhances AI Days	0.107493	0.172599
Mean Contribtion to FDEN over IAH	6%	7%

Table 1. Mean flash densities associated with each set of isolated days, along with their relative contributions to the total flash densities (highlighted in yellow) for each metric box.

forcing, rather the presence of these *key features cannot be directly attributed to the hypotheses under investigation.* Regarding local topography, given a regional map, as in Figure 2b, it is clear that the topography to the north of Galveston Bay is quite complex, with various fingers of Gulf water extending inland in differing directions. This coupled with the proximity of inland lakes and reservoirs, namely Lake Houston approximately 16 km north of the northwestern tip of Galveston Bay (and to a lesser extent Sheldon Reservoir 12 km to the northwest, not depicted in the figure) provide for a favorable environment of enhanced convergence associated with interacting bay and lake breezes capable of explaining the observed flash density enhancements to the east-northeast of the city center. Additionally, this area is primarily classified as that of forest and grassland allowing for a greater latent heat flux, relative to the asphalt coated urban areas.

Overall, enhanced UHI days contribute 25% of the mean flash density over the Houston area, with peak enhancements over the central northern and southern boundaries of the city (Figure 6c; background plus UHI). The result of allowing days in which the SB is active to be included in the analysis, is to primarily enhance the features identified in the background, while contributing upwards of 50% of the lightning surrounding the area of enhanced flash densities extending westward from the southwestern portion of the city (Figure 6d; background plus SB). Isolating enhanced aerosol days, we found that the *overall contributions of enhanced SO_2 days on the mean flash densities over the Houston area to be minimal at best* with mean enhancements over the anomaly area of approximately 7% (Figure 6e; background plus AI).

Based upon the analyses conducted herein, we present the following summary observations:

(1) Devoid of additional forcing offered by the hypotheses outlined in Section 1, certain spatial features persist within the climatology suggesting that the presence of the enhanced flash densities over and northeast (i.e. downwind) of the Houston area are the result of "normal" convective activity tied to areas of preferred convection and local topography, and not the result of anthropogenic enhancements,
(2) Enhanced pollution levels do not appear to have a significant effect on flash densities over the Houston area (i.e. does not support hypothesis 3),
(3) UHI and SB forcing contribute relatively the same amount to the mean flash densities over the Houston area, both tending to enhance the persistent features present in the background climatology on the northeast side of the city (i.e. support for hypotheses 1 and 2).

4. CONCLUSIONS

Utilizing data from three separate archived datasets the hypothesized causative mechanisms behind the documented enhancement in summer season ground flash densities over the Houston area were examined. Findings indicate that the spatial extent of the flash density features are primarily the result of "typical" convective activity tied to the presence of a persistent thermal anomaly over the center of the city, giving rise to a preferential location of convective enhancement,

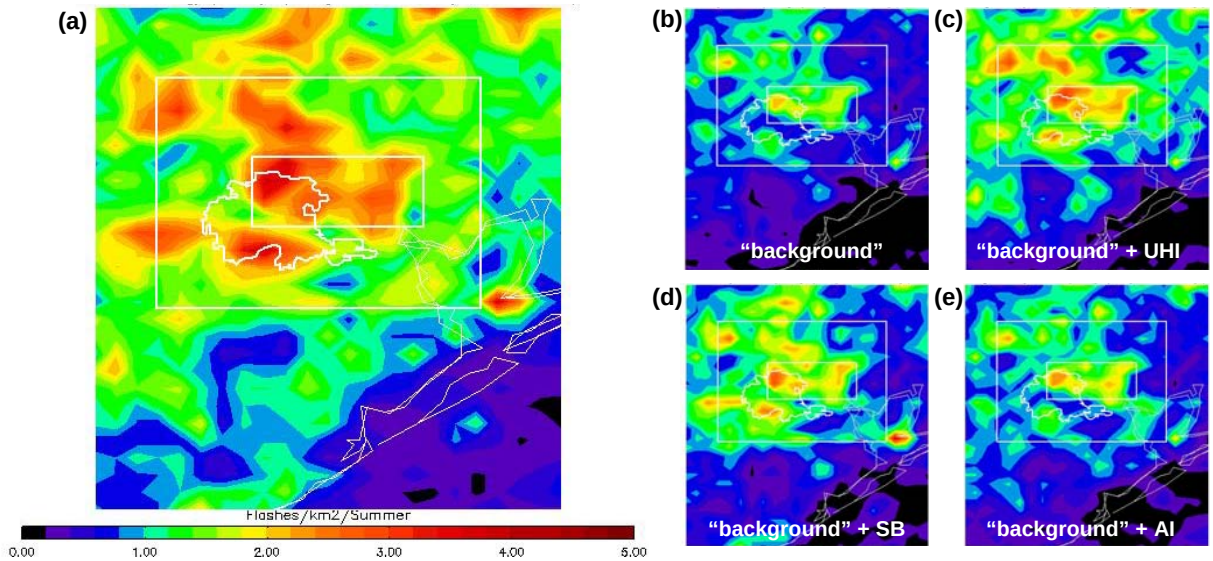

Figure 6. As in Figure 3, spatial variations of mean flash density (valid 0900-1859 CST) for (a) 336 non-contiguous days resulting from the application of SE1 and the first half of SE2, (b) 169 non-enhanced days (following application of SE1-4, as is the case for Figures 6c-e), (c) 169 non-enhanced days plus 57 enhanced UHI days, (d) 169 non-enhanced days plus 62 sea breeze days and (e) 169 non-enhanced days plus 48 enhanced AI days. NOTE: contour shading in all panels correspond to the legend presented in Figure 6a with all panels being normalized 336 days.

coupled with the land surface heterogeneity of the surrounding area. That is not to say that the magnitudes of these features are not enhanced through the hypotheses investigated in this paper, rather that the presence of these *key features cannot be directly attributed to the hypotheses under investigation.*

Relating to the apportionment of cause, based on a climatic viewpoint, we conclude the primary causative mechanisms responsible for the intensity of the Houston CG lightning anomaly to be those associated with hypotheses 1 and 2: specifically that ***UHI thermodynamics*** provide a more favorable environment for convective initiation and thunderstorm intensification as well as contributing to an area of preferred convergence over, and to the east-northeast of the city, with associated ***mesoscale enhancements in sea breeze convergence***. Acting together, these two enhancements cause more frequent convection over the Houston urban area resulting in more lightning activity and heavier precipitation over the city. The dominant of the two, however, remains uncertain as they are both intimately tied to thermal forcing, the common denominator between the two. Regarding the effects of anthropogenic aerosols on enhanced flash densities, from the analyses presented here, it is unclear that enhanced aerosol (CCN) concentrations (in particular, SO_2) have any significant impact on the flash density enhancements under investigation leading us to the conclusion that enhanced aerosol concentrations are the least likely contributor to the climatological enhancements in ground flash density over and around the Houston metropolitan area during the summer season. To the extent that local aerosol contributions are not a primary contributor to regional and/or local lightning maximums, extension of these results to global lightning mapping suggests that stronger emphasis should be placed on regional to local scale circulations and the response of convection and subsequent lightning frequencies to those forcing scales.

5. APPENDIX

In order to explore each of the three aforementioned hypotheses, the merged dataset was filtered so as to control for two of the three variables (sea breeze, large UHI, and/or large AI) while investigating the impacts of the third on CG lightning. Specifically, using the statistical distributions of each variable within the merged dataset, the following quantitative filters were developed (see Appendix for full description):

SE1 - large lightning event day filter
SE2 - sea breeze day filter (includes 6 sub-filters)
SE3 - “large” UHI day filter
SE4 - “large” AI day filter

A.1 Selective Exclusion Filter #1 (SE1) – Large Lightning Event Days.

As previously established, the Houston lightning anomaly is a persistent, non-unique feature along the Gulf Coast, therefore our baseline climatology must be one in which the lightning anomaly persists with the selective exclusion of large events. Here, we have chosen, as in Gauthier et al. 2005, to include a larger domain (as in Figure 1) for the first portions of our selective exclusion analysis. Using the sum of daily flash counts in each of four coastal grid boxes within the domain (see solid black boxes in un-zoomed portion of Figure 1) we used statistics of the summed daily flash count distribution to guide the classification of large event days within our dataset. Due to the skewed, non-Gaussian nature of the flash density distribution, we chose thresholds appropriate to the nature of the flash density histogram based on the cumulative flash density distribution to identify large events. Specifically, large event days were chosen as those days whose 4-box flash count total exceeded 1,930 flashes - the outer fence of the data distribution (defined as the upper-quartile plus 1.5 times the inter-quartile range; Wilkes, 1995). Equivalent to the 90th percentile of the cumulative conditional flash density distribution (conditioned on the presence of lightning in at least one of the four coastal boxes), this method allows for the objective classification of the tail of the distribution as large (coastal) “event days”, of which there were 41.

Application of this first selective exclusion filter (SE1) reduces our dataset to from 527 to 486 overlapping days with large events excluded, from which we note the presence of the persistent flash density anomaly located over the Houston metropolitan area, with a finger of enhanced flash densities extending to the east-northeast (i.e. downwind) of the urban corridor (not shown).

A.2 Selective Exclusion Filter #2 (SE2) – Sea Breeze Day Classification

As a mesoscale feature, the sea breeze can be important in the organization, initiation and/or intensification of coastal convection, therefore knowledge of its occurrence within the dataset is critical. The magnitude of the remaining dataset (486 days) prohibits manual classification of this phenomenon; further, doing so would be subjective with the results not easily reproducible. Arguably however, quantitatively determining the historical incidence of this observable is less than trivial. In this study, we have chosen to use a modified version of the classification algorithm outlined by Borne et al. (1998) who used six observational filters leading to the classification sea breeze days within their dataset.

The filters were developed from empirical studies of the characteristic features of the sea breeze using data from field stations and radiosondes. In the present study, mean hourly wind and temperature data from various CAMS sites (Figure 2) were used to monitor the

diurnal evolution of the wind and thermal fields, while 700 mb data from the NCEP/NCAR Reanalysis was used as a measure for the general synoptic condition (Kalnay et al., 1996).

The first two filters were constructed to exclude days with probable large changes in synoptic conditions, while the third filter excludes days in which synoptic winds are too strong.

F1: change in 700 mb wind direction of less than 90 degrees in the past 12 hours
F2: change in 700 mb wind speed less than 6 m/s in past 12 hours
F3: wind speed < 11 m/s at 18Z (13L)

As the sea breeze is a thermally driven circulation, filter 4 ensures the presence of a reasonably large temperature difference between coastal (CAMS site 8) and inland temperatures (CAMS site 1) for at least 1 hour during the diurnal heating cycle (0700-1800L).

F4: $T_{land(1)} - T_{coast\ (8)} \geq 3^{o}$ C

Applied to our dataset, F1-4 ensure that background conditions are favorable for the development of a sea breeze circulation yielding a total of 239 possible SB days. It is the passage of the remaining two filters (F5 and F6, described below) that will result in the classification of these remaining days as a SB or noSB day.

Given appropriate background conditions (i.e. passage of F1-4), evaluating the behavior of the surface winds during (and following) sea breeze onset is what comprises the final two filters. Specifically, the sea breeze is characterized by a distinct change in surface wind direction of at least 30 degrees resulting in an increased onshore wind component (F5), followed by 5 hours of relatively stable conditions in wind direction (F6). Based on manual inspection, we have chosen to apply the final two filters as follows: CAMS sites 7 and/or 10 must pass the two filters AND CAMS sites 1 and/or 6 must pass the two filters. This approach proves to be rather stringent, requiring a wind shift to occur at two separate locations (along the eastern edge of the metropolitan boundary, as well as further inland – note two sites in the vicinity of each location are used to allow for instances of missing data at one of the sites), however the results provide a high degree of confidence that the filter is correctly classifying SB days.

To evaluate the accuracy of the filter method, 66 of 239 possible SB days (i.e. only considered days in which F1-4 had passed) were manually classified as either SB or noSB days prior to the application of the final two filters (F5 and F6). The filter method selected 40 days as SB days, while the manual classification selected 46 days as SB days out of a total 66 days. Of the 40 days selected by the filter method as SB days, the manual method gave the following results: 35 SB and 5 noSB. These statistics yield a false alarm rate (FAR) of 0.125 indicating that the constructed selection method has an accuracy of greater than 85% in the process of selecting sea breeze days.

Given the accuracy associated with the established methodology, we can further filter our dataset through the application of this filtering process (SE2) from 486 overlapping days (large lightning events excluded) that resulted from the application of SE1 to 215 possible SB days (124 SB and 91 noSB).

A.3 Selective Exclusion Filter #3 (SE3) – Urban Heat Island Classification

Among the many differences between urban and rural areas that have emerged due to urbanization and industrialization, the most notable and well documented is the increase in air temperature in urban areas, called the urban heat island (UHI). A classical definition of a UHI is that of a temperature difference between the urban city and its surrounding rural background (Oke, 1982).

Using hourly temperature data from CAMS sensors each day within our dataset was classified with an index proportional to the intensity of the UHI on that given day. Here, we define the UHI for a given hour as:

$$UHI = \mathbf{T}_{urban(15,24,29)} - \mathbf{T}_{rural(1,5,19)}\ , \qquad (1)$$

where $\mathbf{T}_{urban(15,24,29)}$ is the average hourly mean temperature of CAMS sites 15, 24, and 29 and $\mathbf{T}_{rural(1,5,19)}$ the average hourly mean temperature of surrounding CAMS sites 1, 5 and 19. The CAMS sites chosen for use in the UHI were based on the results of the thermal climatology. Since each of the hypotheses under investigation invoke "forcing-response" relationships (i.e. enhanced UHI forcing results in the atmospheric response of enhanced CG lightning activity) the final UHI associated with each day is taken as the maximum UHI that occurred during the 6 hours preceding the peak in hourly flash counts within the Houston box (solid white box in Figure 1), or 08-14L on non-lightning days.

As with SE1, the statistics, of the daily cumulative UHI distribution guided the objective classification of "Large" UHI days (SE3). Specifically, "Large" UHI days were taken to be those days whose UHI fell within the upper quartile of the cumulative UHI distribution, equivalent to a daily UHI of 4.64 or greater, of which there were 116 of the 486 overlapping days (excluding large lightning days).

A.4 Selective Exclusion Filter #4 (SE4) – Aerosol Classification

As previously discussed, SO_2 was chosen as the aerosol (CCN) tracer for use in this study, with all days in the dataset receiving an Aerosol Index (AI) proportional to the mean SO_2 levels over the industrial center of the Houston metropolitan area. As was the case with the development of the UHI, the SO_2 climatology was used to determine the location and diurnal timing of peak SO_2 concentrations (a proxy for

the location of peak pollution). Here the AI for a given hour is defined as:

$$AI = \mathbf{SO_2}_{(1,6,26)}, \qquad (2)$$

where $\mathbf{SO_2}_{(1,6,26)}$ is the average of the hourly mean SO_2 concentration measured at CAMS sites 1, 6 and 26. Similar to the UHI, a "forcing-response" relationship is applied, with the final AI associated with each day taken as the average (vice maximum) of the aerosol indices during the 6 hours preceding the peak in hourly flash counts within the Houston box (08-14L on non-lightning days).

Again, statistics of the daily cumulative distribution guided the objective classification of "Large" event days. Here, "Large" AI days (SE4) were taken to be those days whose AI fell within the upper quartile of the cumulative AI distribution, equivalent to a daily AI of 7.1 or greater, of which there were 121 of the 486 overlapping days (excluding large lightning days).

Acknowledgments. Post-processed lightning data were provided by the *NASA Lightning Imaging Sensor (LIS) instrument team and the LIS data center via the Global Hydrology Resource Center (GHRC) through a license agreement with Global Atmospherics, Inc (GAI).*

6. REFERENCES

Barnes, S. L., 1964: A Technique for Maximizing Details in Numerical Weather Map Analysis. *Journal of Applied Meteorology,* **3**(4), 396–409.

Borne, K., D. Chen, and M. Nunez, 1998: A method for finding sea breeze days under stable synoptic conditions and its application to the Swedish west coast, *Int. J. Climate*, **18**, 901-914.

Bornstein, R., and Q. Lin, 2000: Urban heat islands and summertime convective thunderstorms in Atlanta: three case studies. *Atmos. Environ.,* **34**, 507-516.

Braham, R. R., R. G. Semonin, A. H. Auer, S. A. Changnon, Jr., and J. M. Hales, 1981: Summary of urban effects on clouds and rain. METROMEX: A review and summary. *Meteorological Monographs, Amer. Meteorol. Soc.,* **40**, 141-152.

Continuous Ambient Monitoring Stations (CAMS), 2005: http://www.tceq.state.tx.us/compliance/monitoring/cams.html

Cummins, K. L., M. J. Murphy, E. A. Bardo, W. L. Hiscox, R. B. Pyle, A. E. Pifer, 1998: A combined TOA/MDF technology upgrade of the U.S. National Lightning Detection Network, *J. Geophys. Res.,* **103**(D8), 9035-9044.

Gauthier, M. L., W. A. Petersen, L. D. Carey, and R. E. Orville, 2005: Dissecting the anomaly: A closer look at the documented urban enhancement in summer season ground flash densities in and around the Houston area, *Geophys. Res. Lett.,* **32**, L10810, doi:10.1029/2005GL022725.

Hjelmfelt, M. R., 1982: Numerical simulation of the effects of St. Louis on mesoscale boundary layer airflow and vertical air motion: simulations of urban vs. nonurban effects. *J. Appl. Meteor.*, **21**, 1239-1257.

Huff, F. A., and S. A. Changnon, Jr., 1973: Precipitation modification by major urban areas. *Bull. Amer. Meteor. Soc.,* **54**, 1220-1232.

Jauregui, E., and E. Romales, 1996: Urban effects on convective precipitation in Mexico City. *Atmos. Environ.,* **30**, 3383–3389.

Kalnay, E., M. Kanamitsu, R. Kistler, W. Collins, D. Deaven, L. Gandin, M. Iredell, S. Saha, G. White, J. Woollen, Y. Zhu, A. Leetmaa, B. Reynolds, M. Chelliah, W. Ebisuzaki, W. Higgins, J. Janowiak, K.C. Mo, C. Ropelewski, J. Wang, Roy Jenne and Dennis Joseph. 1996: The NCEP/NCAR 40-Year Reanalysis Project**.** *Bull. Amer. Meteor. Soc.*:**77**, 437–471.

Naccarato K. P., O. Pinto Jr., I. R. C. A. Pinto, 2003: Evidence of thermal and aerosol effects on the cloud-to-ground lightning density and polarity over large urban areas of Southeastern Brazil, *Geophys. Res. Lett.,* **30** (13), 1674, doi:10.1029/2003GL017496.

Oke, T. R., 1982: The energetic basis of the urban heat island. *Quart. J. Roy. Meteor. Soc*., **108**, 1-24.

Orville, R. E., G. R. Huffines, J. Nielsen-Gammon, R. Zhang, B. Ely, S. Steiger, S. Phillips, S. Allen, W. Read, 2001: Enhancement of cloud-to-ground lightning over Houston, Texas, Geophys. Res. Lett., **28**(13), 2597-2600.

Rosenfeld, D., 1999: TRMM observed first direct evidence of smoke from forest fires inhibiting rainfall, *Geophys. Res. Lett.*, **26**, 3105–3108.

Rosenfeld, D., 2000: Suppression of rain and snow by urban and industrial air pollution, *Science*, **287**, 1793– 1796.

Rosenfeld, D., and M. I. Lensky, 1998: Space-borne based insights into precipitation formation processes in continental and maritime convective clouds, *Bull. Am. Meteorol. Soc.*, **79**, 2457–2476.

Rosenfeld, D., and W. L. Woodley, 2000: Convective clouds with sustained highly supercooled liquid water down to -37.5°C, *Nature*, **405**, 440–442.

Rosenfeld, D., and W. L. Woodley, 2003: Spaceborne inferences of cloud microstructure and precipitation processes: synthesis, insights and implications, *Cloud Systems, Hurricanes, and the Tropical Rainfall Measuring Mission (TRMM) – A tribute to Dr. Joanne Simpson*, Eds. W-K Tao and R. Adler, *Meteorological Monographs*, Vol. 29, No. 51, Amer. Meteorol. Soc., pp. 59-80.

Shepherd J. M., H. F. Pierce, and A. J. Negri, 2002: Rainfall modification by major urban areas: Observations from spaceborne radar on the TRMM satellite. *J. Appl. Meteor*., **41**, 689-701.

Soriano, L. R., and F. Pablo, 2002: Effect of small urban areas in central Spain on the enhancement of cloud-to-ground lightning activity, *Atmos. Env.*, **36**(17), 2809-2816.

Steiger S. M., R. E. Orville, and G. R. Huffines, 2002: Cloud-to-ground lightning characteristics over Houston, Texas: 1989–2000, J. Geophys. Res., **107** (D11).

Wacker, R. S., R. E. Orville, 1999a: Changes in measured lightning flash count and return stroke peak current after the 1994 U.S. National Lightning Detection Network upgrade: 1. Observations, J. Geophys. Res., **104**(D2), 2151-2158.

Wacker, R. S., R. E. Orville, 1999b: Changes in measured lightning flash count and return stroke peak current after the 1994 U.S. National Lightning Detection Network upgrade: 2. Theory, J. Geophys. Res., **104**(D2), 2159-2162.

Westcott, N. E., 1995: Summertime Cloud-to-Ground Lightning Activity around Major Midwestern Urban Areas. *Journal of Applied Meteorology*: Vol. 34, No. 7, pp. 133–1642.

Wilkes, D. S., 1995: Statistical methods in the Atmospheric Sciences. *Academic Press*, 465 pp.

Williams, E., D. Rosenfeld, N. Madden, J. Gerlach, N. Gears, L. Atkinson, N. Dunnemann, G. Frostrom, M. Antonio, B. Biazon, R. Camargo, H. Franca, A. Gomes, M. Lima, R. Machado, S. Manhaes, L. Nachtigall, H. Piva, W. Quintiliano, L. Machado, P. Artaxo, G. Roberts, N. Renno, R. Blakeslee, J. Bailey, D. Boccippio, A. Betts, D. Wolff, B. Roy, J. Halverson, T. Rickenbach, J. Fuentes, and E. Avelino, 2002: Contrasting convective regimes over the Amazon: Implications for cloud electrification. *J. Geophys. Res.*, **107**, D20, 8082, doi:10.1029/2001JD000380.